Original Article

Optimized Bilosome Delivery System for Dasatinib: Formulation, Characterization, and Pharmacokinetic Evaluation

Ahmed Hamed Salman, Shaimaa Nazar Abd Alhammid

DOI: 10.34172/PS.026.43430

To appear in: Pharmaceutical Science (https://pstbzmed.com/)

Received date: 28 Oct 2025

Revised date: 6 Jan 2026

Accepted date: 7 Jan 2026

Please cite this article as: Salman AH, Alhammid SNA. Optimized bilosome delivery system for dasatinib: Formulation, characterization, and pharmacokinetic evaluation. Pharm Sci. 2026. doi: 10.34172/PS.026.43430

Optimized bilosome delivery system for dasatinib: formulation, characterization, and pharmacokinetic evaluation

Running Title

Bilosome-based strategy for dasatinib bioavailability

Authors

Ahmed Hamed Salman [1,2*], Shaimaa Nazar Abd Alhammid [2]

[1] Department of Pharmaceutics, College of Pharmacy, Al-Bayan University, Baghdad, Iraq

[2] Department of Pharmaceutics, College of Pharmacy, University of Baghdad, Baghdad, Iraq

Corresponding author

Name: Ahmed Hamed Salman

Email: ahmed.s@albayan.edu.iq

https://orcid.org/0000-0001-7343-2064

Abstract

Background: Dasatinib (DST), a second-generation tyrosine kinase inhibitor, suffers from poor aqueous solubility and pH-dependent absorption, limiting its oral bioavailability. Bilosomes—vesicular carriers stabilized with bile salts—offer enhanced stability in the gastrointestinal tract and improved drug encapsulation compared to conventional liposomes and niosomes. In this study, a DST-loaded bilosome (DST-LB) formulation was developed and its solubility, dissolution, and bioavailability were evaluated.

Methods: Bilosomes were prepared using the reverse-phase evaporation method and optimized via Box–Behnken design. The formulation was characterized for particle size, zeta potential, entrapment efficiency, micromeritic properties, and morphology. Capsules were evaluated for weight variation, content uniformity, dissolution, and stability. Pharmacokinetic studies were conducted in rabbits and analyzed using non-compartmental modeling.

Results: The optimized bilosomes exhibited a mean particle size of 113 nm, a polydispersity index of 0.11, a zeta potential of –22 mV, and an entrapment efficiency of 81%. Capsules showed excellent flowability and uniformity. Dissolution studies showed a sustained-release profile

governed by non-Fickian transport (n = 0.725), whereas the marketed tablet displayed a faster release profile following first-order kinetics (n = 0.450). In vivo, bilosomes achieved higher C_{max} (477.8 ng/mL vs. 374.4 ng/mL), shorter Tmax (1 h vs. 1.5 h), and greater AUC (2886.5 ng · h/mL vs. 2107.7 ng·h/mL), indicating that the systemic exposure was 38% higher with bilosomes compared to the marketed tablet. Stability testing confirmed first-order degradation with a predicted shelf life of 2.1 years.

Conclusions: DST-LB significantly enhanced dissolution, absorption, and bioavailability compared to the marketed tablet, supporting their potential as a modified-release oral delivery system for improved therapeutic outcomes.

Keywords

Dasatinib, Nanoparticles, pharmacokinetics, Drug Delivery Systems, Bile Acids and Salts, Bioavailability

1. Introduction

Dasatinib monohydrate (DST) is a second-generation tyrosine kinase inhibitor indicated for patients with chronic myeloid leukemia (CML) who exhibit resistance or intolerance to prior therapies.[1] Aqueous solubility is believed to contribute substantially to variability in medication absorption [2]. DST is rapidly absorbed, achieving peak plasma concentrations within 0.5 to 3 hours after oral administration, with solubility contingent upon pH levels.[3] The inadequate bioavailability of DST may be attributed to its limited aqueous solubility, as it is classified as a BCS Class II compound. The bioavailability of BCS class II medicines is based on solubility and dissolution.[4]

In vitro findings demonstrate that DST exhibits pH-dependent solubility. Solubility diminishes significantly at pH levels over 4.0, declining from 18.4 mg/mL at pH 2.6 to 0.205 mg/mL at pH 4.28, and further to <0.001 mg/mL at pH 6.99.[5] Thus, considerable pharmacokinetic interactions have also been reported between tyrosine kinase inhibitors and medications that elevate stomach pH. The co-administration of DST with famotidine and antacids resulted in a decrease in AUC of around 60% and 55%, respectively.[5] A similar interaction was reported with omeprazole.[6] Consequently, H2 antagonists and proton pump inhibitors are not advised for simultaneous administration with DST [7]. In addition to medication interactions,

reduced absorption of DST may occur under pathophysiological conditions that elevate stomach pH, such as hypochlorhydria or achlorhydria, which is prevalent in the population, with its incidence rising with age.[8] Overcoming such shortcomings has gained attention in recent years to improve the oral bioavailability of DST. One of these attempts was to use an amorphous solid dispersion,[9-11] nanoemulsifying drug delivery system[12], nanoparticles.[13,14]

Bilosomes, which are vesicles stabilized by bile salts, constitute a novel vesicular carrier.[15] They function as closed vesicles comprised of nonionic surfactants that resemble niosomes but incorporate bile salts.[16] When taken orally, bilosomes offer protection against challenging circumstances, including the stomach's acidic environment and digestive enzymes, due to the inclusion of bile salts as their primary structural component.[17] Moreover, they provide superior durability against the challenging environments of the gastrointestinal tract for the encapsulated therapeutic agent, in contrast to conventional niosomes and liposomes, which rapidly degrade and release the encapsulated medication before reaching the target cells.[18] Bilosomes exhibit remarkable durability at ambient temperatures and within refrigeration, primarily due to the large negative charge conferred by bile salts. From a commercial perspective, bilosomes may be favored over alternative nanocarrier systems because of their accessibility and the simplicity and cost-effectiveness of their manufacturing processes. Moreover, this approach offers improved patient adherence.[19-21] Bilosomes primarily consist of phospholipids (in liposomes) or nonionic surfactants (in niosomes), cholesterol, and bile salts.[22] The ratios of these substances vary according to the characteristics of the encapsulated medicine and the desired method of administration. The structural components are essential for the effective production of bilosomes with the requisite properties.[23]

Despite exploring multiple formulation strategies to improve DST’s oral bioavailability, these methods have shown limited success in overcoming pH-dependent solubility and drug–drug interactions with acid-reducing agents. Most previous studies mainly focused on enhancing dissolution rates but did not adequately address DST's instability in the gastrointestinal tract or its variable absorption under altered gastric conditions. Additionally, conventional nanocarriers such as liposomes and niosomes often suffer from premature degradation, poor stability, and rapid drug leakage, limiting their translational potential. This creates a critical need for a robust,

stable, and patient-friendly oral delivery system that can protect DST from gastric degradation, sustain its release, and improve systemic absorption. Bilosomes, with their bile salt–stabilized vesicular structure, directly meet this need by offering increased stability, resistance to enzymatic degradation, and enhanced intestinal absorption, making them a promising alternative to conventional nanocarriers.

This study aims to develop, optimize, and evaluate a bilosome-based oral delivery system for DST that specifically tackles its poor aqueous solubility, pH-dependent absorption, and instability in the gastrointestinal tract. By adding bile salts and Soluplus® into the bilosome structure, the formulation is intended to enhance drug solubilization, shield against gastric degradation, and increase systemic exposure compared to the marketed tablet.

2. Methods

2.1. Materials

The materials employed in this study include cholesterol from Avonchem, UK; methanol (99%) from CHEM-lab, Belgium; mannitol; potassium dihydrogen phosphate, phosphate-buffered saline (pH 7.4), and sodium hydroxide, all sourced from Hi-Media, India; and sodium deoxycholate from Avonchem Ltd., UK; Triton-X100 purchased from Loba Chemie Pvt. Ltd., India.

Additional reagents comprise Span® surfactants 20, 40, 60, and 80, as well as Tween® surfactants 20, 40, 60, and 80, both from Loba Chemie Pvt. Ltd., India; dasatinib monohydrate powder from Wuhan Hanweishi Pharmchem Co., China; Soloplus® from Germany; and ethanol (96%), dimethyl formamide, and hydrochloric acid (HCl), all provided by CHEM-lab, Belgium.

2.2. Determination of Absorption Maxima (λ_{max})

The UV spectra were acquired using a double-beam UV/Visible spectrophotometer (Shimadzu UV-19001, Japan) with 10 mm matched quartz cells. The solution contains 100 mg of the drug per 100 mL dissolved in different solutions [24,25].

2.3. Preparation and formulation of dasatinib-loaded bilosome (DST-LB) nanoparticle formulation

The reverse-phase evaporation method was used to formulate the DST-LB formulas with some modification; the components of DST-LB must include cholesterol, nonionic surfactant (Tweens and spans), bile salts (sodium deoxycholate (SDC)), and stabilizing agents (soluplus) [26-28]. The procedure is as follows: a mixture of surfactants (Tween 60 (150 mg) and Span 60 (110.083 mg)), 95.1515 mg of cholesterol, and 20 mg of DST was combined in a round-bottom flask with an adapter containing 10 mL of ethanol. The solution was sonicated in a water bath sonicator (Copley Scientific Limited, Nottingham, England) at 40°C for 15 minutes to ensure complete solubilization of the mixture. The aqueous phase solution was made by dissolving 12.2727 mg of SDC and 100 mg of Soluplus in 5 mL of deionized water. The phases were mixed using an ultrasonic bath (Copley Scientific Limited, Nottingham, England) to form a stable white emulsion. The emulsion was then dried using a rotary evaporator at 150 rpm (150 mbar, 40°C) for 60 minutes to form a thin film, and subsequently rehydrated with 10 mL of deionized water. The resulting bilosome dispersion (2 mg/mL) was heated in a water bath sonicator (Copley Scientific Limited, Nottingham, England) at 40°C for 30 minutes to create a homogeneous dispersion, followed by sonication (VCX 750, VibraCell™ Sonicator, Sonics & Materials Inc., USA) for 5 minutes at 30% amplitude with a pulse of 10 seconds on and 10 seconds off. This procedure was employed to minimize vesicle size, after which the resulting dispersion was stored at 4 °C for subsequent analyses. For details on the pilot study concerning the optimization and selection of DST-LB formulation components, refer to **Supplementary File S1**.[29]

2.4. Lyophilization of the optimized formula

Lyophilization of the optimized bilosomes formula was performed using mannitol as a cryoprotectant (2 w/v%). The lyophilization process involved subjecting the formulation to a primary freezing temperature of -20 °C for 24 hours, followed by immersion in liquid nitrogen for 15 minutes. Subsequently, the formulation was lyophilized for 72 hours under a pressure of 0.4 bar [30,31]. The obtained powder was stored in a tightly closed container for further investigations.

2.5. Characterization of DST-LB formulation

2.5.1. Measurement of particle size, polydispersity index, and zeta potential

Dynamic light scattering (DLS) was used to determine the polydispersity index (PDI) and polydispersity of DST-LB using a Zetasizer (Malvern, UK). The measurements were conducted at 25 ± 2°C [27,32]. Additionally, the zeta potential (ZP) of the bilosomes was measured by observing how the bilosomes moved in an electrical field in deionized water using the same instrument. To ensure accurate measurements, the samples were diluted 10-fold with deionized water before analysis. The ZP measurement allowed an understanding of the surface charge of the bilosomes, which was important for the stability of the bilosomes.[33,34]

2.5.2. Determination of percentage entrapment efficiency

The direct method (dialysis method) was used to calculate the EE; a 2 mL DST-LB formula was placed in a dialysis bag (HiMedia Laboratories LLC, USA) and dialyzed against 500 mL of medium (deionized water + 0.5% Triton X). After 24 hours, the amount of drug recovered from the dialysis bag (Wr) was determined by UV-vis spectroscopy. The EE was calculated using the equation below[35]:

$$EE(\%) = \frac{W_r}{W_{total}} \times 100\%$$

Where W_{total} is the total amount of drug in the dialysis bag before the procedure, W_r is the amount of drug that was recovered from the dialysis bag at the end.

2.5.3. Transmission Electron Microscopy (TEM)

Zeiss Libra 120 PLUS (Carl Zeiss NTS, Germany) was used for all TEM investigations of bilosome morphology and bilayer architecture. A freshly prepared optimized bilosome suspension was diluted with deionized water (1 mg/mL), and then the suspension was filtered. The diluted suspension was sonicated for 5 minutes in an ice-cooled bath to disperse aggregates, and the suspension was maintained on ice until grid deposition. Continuous carbon-coated, 200-mesh copper grids were glow-discharged (15 mA, 30 s) to render the surface hydrophilic. A 3 µL aliquot of nanobilosome suspension was applied and adsorbed for 60 s. Excess liquid was wicked away with filter paper. Then, 5 µL of 2% (w/v) uranyl acetate (pH 4.5) was added for 30 sec. Grids

were blotted, air-dried under dust-free conditions for 10 min, and loaded immediately into the microscope. Digital micrographs were recorded with minimal beam dose to prevent radiation damage. Five randomly selected grid squares were imaged per sample to ensure representative morphology [36].

2.6. Preparation of the precapsulation powder of DST-LB

The lyophilized powder, weighing 687.52 mg and containing an equivalent dose of 20 mg of DST, was carefully formulated by adding excipients to enhance encapsulation. Specifically, 10% (68.75 mg) of microcrystalline cellulose (Avicel® PH 102, IFF Pharma Solutions, Delaware, USA) was included to enhance flowability, 2% (13.75 mg) of croscarmellose sodium (Ac-Di-Sol®, IFF Pharma Solutions, Delaware, USA) was added as a superdisintegrant to promote rapid breakdown upon administration, and 1% (6.88 mg) of magnesium stearate (Ligamed®, Peter Greven GmbH & Co. KG, Bad Münstereifel, Germany) served as a lubricant to simplify capsule filling. The final mixture, totaling 776.90 mg, was deemed suitable for encapsulation in hard gelatin capsules (000 capsules) for oral delivery.

2.7. DST dose calculation for animal study

For current research purposes, the human oral dose of DST at 1.67 mg/kg/day (typical for chronic phase CML) can be converted to a rabbit equivalent using the FDA's body surface area (BSA) method. With K_m values of 37 for humans and 12 for rabbits, the calculation yields an animal equivalent dose of approximately 5.1 mg/kg/day for rabbits.[37]

2.8. Animal housing and care

The study was approved by the Research Ethics Committee of the University of Baghdad, College of Pharmacy, with approval number "RECAUBCP22202505A," dated September 22, 2024. The study follows the principles of the Office International des Épizooties on animal ethics. The methods used on the animals fully comply with regional and international regulations governing the ethical treatment and use of laboratory animals. The authors complied with the ARRIVE 2.0 guidelines.[38]

The rabbits were sourced from the animal facility at the College of Veterinary Medicine, University of Baghdad, and they were given a minimum of 7 days to acclimate before beginning

the experiments.[39] During the acclimation phase, the rabbits were housed in hygienic plastic cages in a controlled laboratory environment maintained at 21–24°C and with humidity ranging from 50% to 60%. They experienced a 12-hour light/dark cycle and had unlimited access to a standard diet, along with fresh water throughout the duration of the study.[40] All animals received environmental enrichment and humane care in line with the institution's established guidelines.

2.9. Analytical HPLC

A validated reverse-phase HPLC method was employed for the quantitative determination of DST in rabbit plasma, using montelukast as the internal standard. Sample preparation involved protein precipitation with acetonitrile, followed by centrifugation and injection of the supernatant. Chromatographic separation was achieved on a C18 column (150 × 4.6 mm, 5 µm particle size) under isocratic conditions with a mobile phase of acetonitrile and 0.1% formic acid in water (60:40, v/v). The flow rate was maintained at 1.0 mL/min, with an injection volume of 50 µL. Detection was performed using a UV detector at 320 nm, ensuring clear resolution of analyte and internal standard peaks. Calibration curves (5–500 ng/mL) were constructed by plotting the ratio of DST to internal standard peak areas against known concentrations. The method was validated for specificity, linearity ($r^2 \geq 0.999$), accuracy, precision, recovery, and sensitivity in accordance with US-FDA/ICH bioanalytical guidelines.[41-43]

2.10. Pharmacokinetic evaluation (*in vivo* study)

A validated method was used to conduct a pharmacokinetic study of DST in two groups of male New Zealand White rabbits, each group comprising 10 animals weighing 1.5-2.0 kg. Before dosing, the rabbits fasted overnight. DST was administered orally at a dose of 5.1 mg/kg. One group received the standard DST tablet (Sprycel, Bristol-Myers Squibb, USA), and the other group received the DST-LB formulation. Blood samples (0.5 mL) were collected from the marginal ear vein at baseline (pre-administration) and at multiple time points post-dose: 0.25, 0.5, 0.75, 1, 1.5, 2, 2.5, 3, 4, 6, 8, 10, 12, and 24 hours. Following collection, blood samples were centrifuged for 10 minutes at 4000 rpm to isolate plasma, which was subsequently stored at -40°C.

Using the PKSolver 2.0 application, non-compartmental models were employed to determine pharmacokinetic parameters.[44] The obtained AUC is a unique parameter for estimating bioavailability. The pharmacokinetic profile of DST is characterized by several key parameters, including the maximum serum concentration (C_{max}), which denotes the peak plasma level achieved after administration, the time to reach this peak (T_{max}), and the time to reach 50% plasma concentration ($t_{0.5}$). Additionally, the area under the plasma concentration-time curve (AUC) provides a quantitative measure of overall drug exposure. Specifically, AUC_{0-t} and $AUC_{0-\infty}$ calculated using the trapezoidal rule. These parameters collectively facilitate a comprehensive understanding of the drug's absorption kinetics.[45]

2.11. Statistical analysis

Statistical analyses were performed using GraphPad Prism 10.5. Experimental data are presented as mean ± standard deviation. For the solubility study comparison, the Brown-Forsythe ANOVA test with post hoc Dunnett's T3 multiple comparisons was used to analyze differences in solubility between groups for non-parametric variables. To assess differences between groups in particle size, PDI, drug content, and EE, a one-way ANOVA with post hoc Holm-Šídák's multiple comparisons test was employed, as the data followed a normal distribution. The level of significance was <0.05.

3. Results

3.1. Optimization of DST-LB formulation

In the current study, optimization was carried out using the Box-Behnken design (BBD), with a total of 46 formulas evaluated across five factors (3^5) at three levels (see Table S1). Table S2 illustrates the results of each formula in terms of response parameters (PS, EE, and PDI), in which PS ranged from 89.8±1.5 to 314.3±1.9 nm, PDI ranged from 0.05±0.001 to 0.52±0.01%, and EE ranged from 0.73±0.004 to 0.95±0.02%. Refer to **Supplementary File S1**.

The optimized formula was selected via numerical optimization in Minitab 17.1.0, based on the desirability factor's proximity to 1. The predicted cholesterol (x1 = 112.5 mg), Tween 60 (x2 = 150 mg), Span 60 (x3 = 97.6 mg), SDC (x4 = 13.9 mg), and Soluplus (x5 = 100 mg) were

acquired, and this was selected as the optimized formula with a desirability of 0.9946, as seen in **Figure S1**.

3.2. Characterization of DST-LB formulation

3.2.1. Particle size and PDI

The Z-average, or the average particle size, was measured to be 113.2 ± 0.6 nm, as illustrated in Figures 1A and 1B. The PDI measures the uniformity of particle sizes within the formulation. The actual PDI is 0.11 ± 0.2, as illustrated in Figure 1C.

3.2.2. Zeta potential

The zeta potential measures the surface charge of the particles, which affects their stability. The actual zeta potential is -22.36 ± 1.21mV. A negative zeta potential indicates that particles are likely to repel each other, thereby contributing to the formulation's stability, as illustrated in Figures 1D and 1E.

3.2.3. Entrapment efficiency

Entrapment efficiency refers to the percentage of DST successfully encapsulated within the bilosomes. The entrapment efficiency is 81.0 ± 2.1%.

3.2.4. TEM studies

The optimized formula exhibits uniform, spherical vesicle morphology, confirming successful bilayer self-assembly. Additionally, the images show unilamellar vesicles from multilamellar structures, as seen in Figures 1F and 1G.

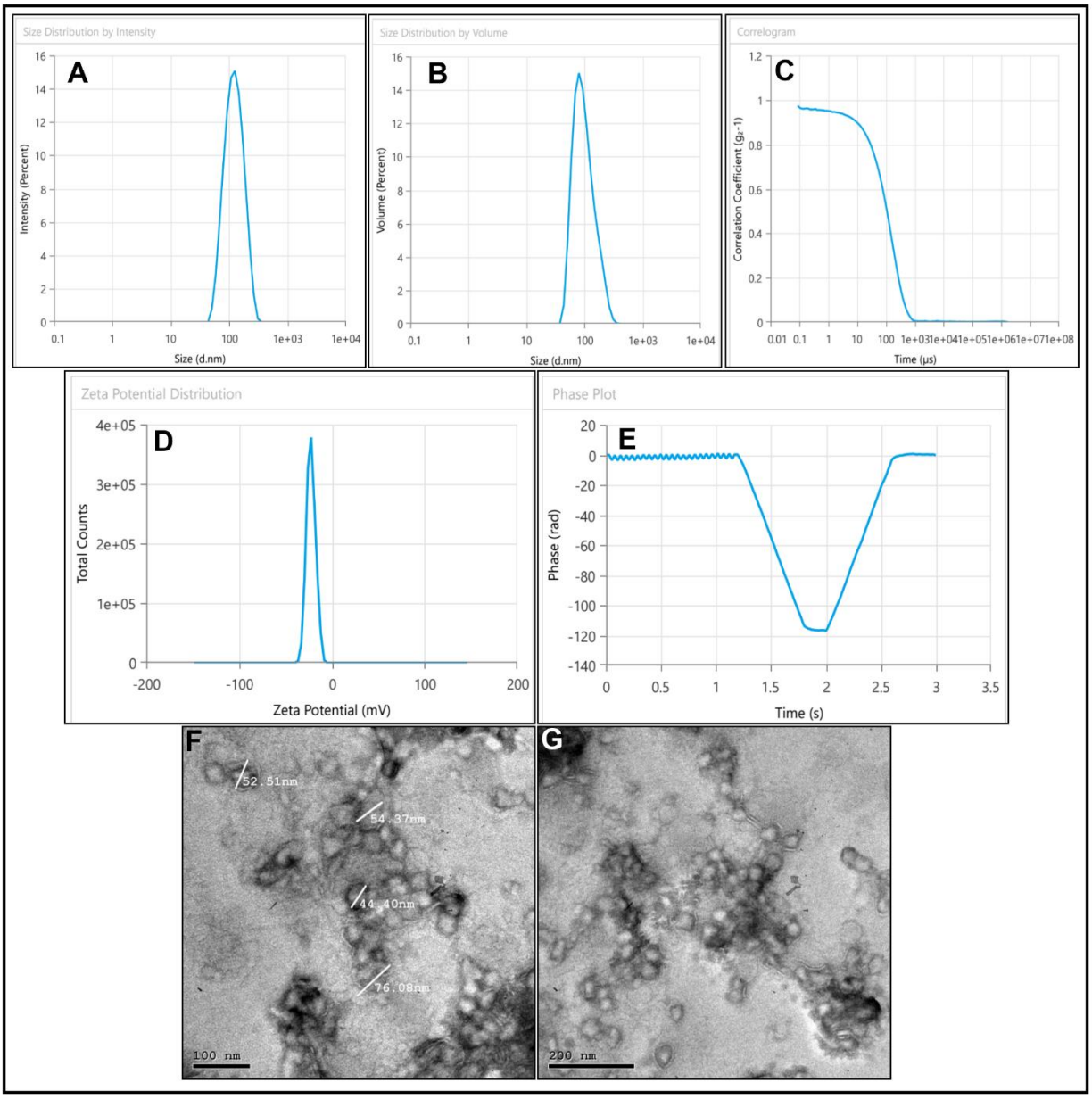

Figure 1: Characterization of the selected DST-LB formula. (A & B) Particle size, C) polydispersity index, (D & E) Zeta potential, (F &G) TEM of the optimized bilosomal formulation containing DST at two magnifications at 100 nm bar scale, and 200 nm bar scale.

3.3. *In vitro* dissolution test

The dissolution study revealed distinct differences between the DST-LB capsule formulation and the marketed DST tablet. The marketed tablet exhibited a rapid onset of drug release, with approximately one-third of the drug released within the first five minutes and more

than 80% released by 30 minutes. By 40 minutes, dissolution exceeded 90%, thereby fulfilling the USP acceptance criterion for immediate-release dosage forms, which requires not less than 80% of the labeled amount to be dissolved within 30 minutes. In contrast, the DST-LB capsule demonstrated a slower release profile. No drug release was detected at five minutes, and only about half of the drug was released by 20 minutes. At 30 minutes, the capsule achieved approximately 71% release, falling short of the USP threshold. The complete release was approached only after 50–60 minutes, indicating a delayed but ultimately near-complete dissolution. These findings suggest that while the marketed tablet is optimized for rapid systemic availability, the bilosome DST-LB capsule provides a more gradual release profile, which may be advantageous in contexts where sustained plasma concentrations are desirable (Figure 2).

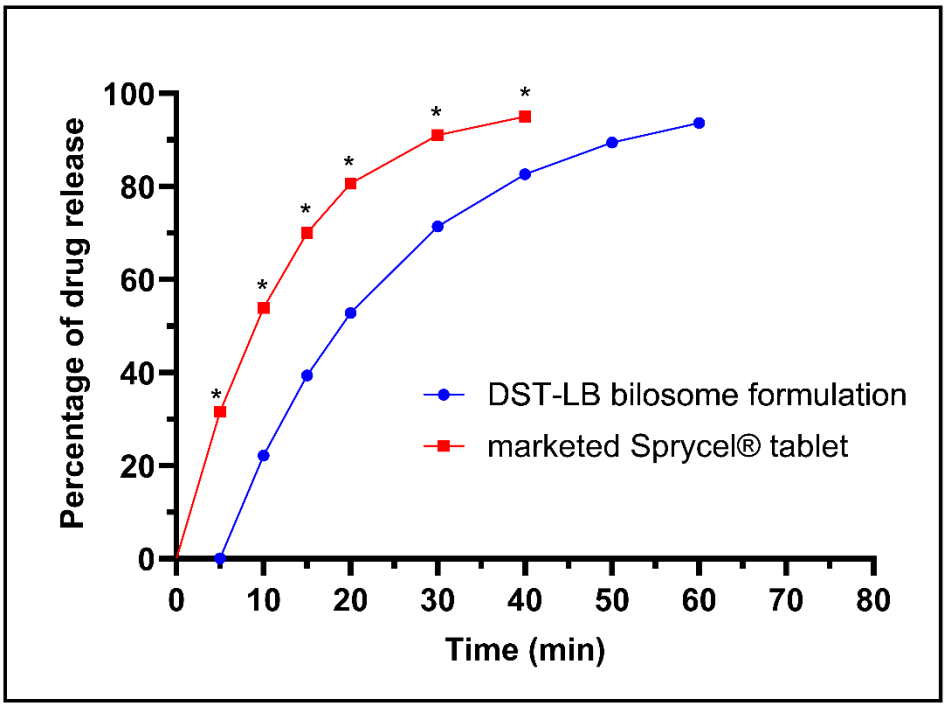

Figure 2: The in vitro dissolution test results of the DST-LB capsule compared to the marketed tablet (* indicates significant differences, i.e., p-value <0.05 between capsule and tablet)

Kinetic modeling further clarified the release mechanisms of the two formulations. For the DST-LB capsule, the dissolution data were best described by a first-order model ($R^2 = 0.94$), indicating that the release rate was concentration-dependent. Secondary fits to the Korsmeyer–

Peppas model indicated a non-Fickian transport mechanism combining diffusion and erosion. The calculated diffusional exponent (n) for the DST-LB capsule was 0.725, a value greater than 0.5, which is indicative of non-Fickian transport. This finding supports the interpretation that a combination of diffusion governs drug release from the DST-LB capsule, driven by the bilayered structure and the carrier matrix's erosion. In contrast, the marketed tablet exhibited an almost perfect first-order fit (R^2 = 0.9986), indicating a highly predictable, rapid dissolution process dominated by concentration-driven release. The diffusional exponent (n) for the marketed tablet was 0.450, a value close to the theoretical Fickian diffusion threshold, suggesting that drug release is primarily governed by simple diffusion processes consistent with immediate-release dosage forms. The strong correlation with first-order kinetics underscores the tablet's immediate-release nature, in line with compendial expectations, as shown in Table 1.

Table 1

Taken together, these results highlight the divergent release behaviors of the two formulations. The marketed tablet conforms to USP monograph specifications for immediate-release DST, ensuring rapid bioavailability and therapeutic onset. The DST-LB capsule, although not meeting the immediate-release criteria, demonstrates a controlled release profile characterized by non-Fickian transport and a higher diffusional exponent. This mechanistic distinction suggests that the capsule could be strategically valuable in clinical settings requiring prolonged exposure or reduced dosing frequency. From a regulatory perspective, the capsule would be more appropriately classified as a modified-release dosage form, necessitating evaluation under distinct USP criteria and further in vitro–in vivo correlation studies to establish its therapeutic relevance.

3.4. Stability studies

The optimized formula underwent accelerated stability testing at three different temperatures (25°C, 40°C, and 50°C) over 12 weeks, showing degradation rate constants (k) of 9.69E-04, 7.26E-03, and 2.50E-02 $week^{-1}$, respectively. Figure 3 displays the logarithm of the percent remaining of dastanib as a function of time (in weeks) at each temperature. The obtained

profiles were linear (a line did not deviate from linearity), indicating that DST degradation follows first-order kinetics. The expiration date at 25°C was 2.09 years.

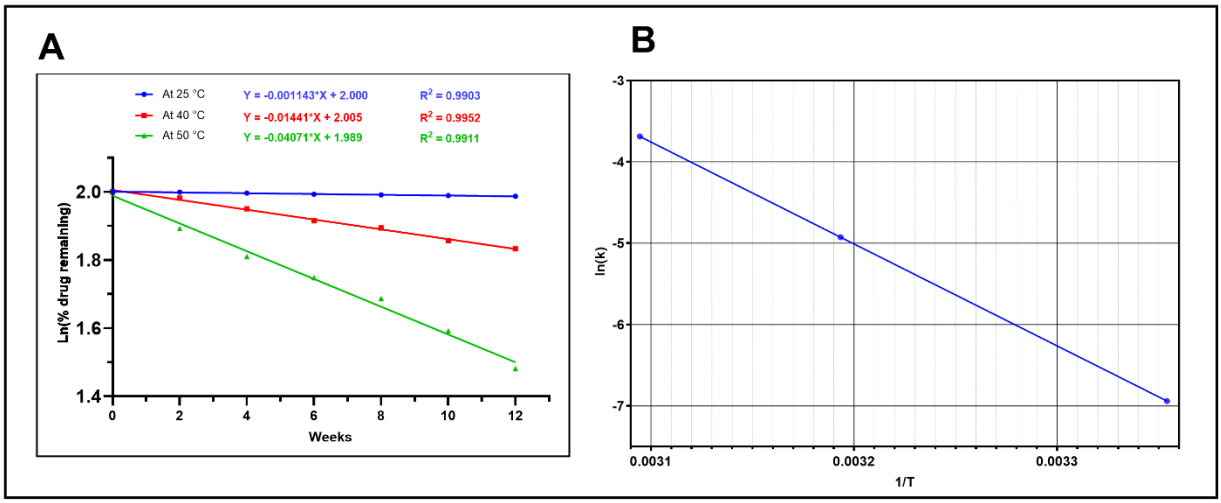

Figure 3: Degradation profile of DST in the optimized formula in the capsule at different accelerated temperatures. A) Represent the actual degradation profile at 25, 40, 50 °C. B) Arrhenius plot based on the full 40 °C and 50 °C stability study.

3.5. Pharmacokinetics study

Table 2 compares the pharmacokinetic parameters of two DST formulations: the standard tablet and the DST-LB. The bilosome formulation demonstrates a shorter half-life (3.69 hours vs. 4.38 hours) and faster absorption, reaching maximum concentration in 1 hour compared to 1.5 hours for the standard tablet. Additionally, the DST-LB achieves a higher maximum concentration (477.78 ng/mL) and greater overall exposure, as indicated by higher AUC values for both the 0 – 24 hour period (2851.79 ng/mLh vs. 2061.72 ng/mLh) and to infinity (2886.49 ng/mLh vs. 2107.67 ng/mLh). Its relative bioavailability is also increased, with AUC values of 138.30% and 136.95%. Overall, the DST-LB exhibits faster absorption, higher peak concentration, and improved bioavailability compared to the standard tablet, as shown in Figure 4.

Table 2

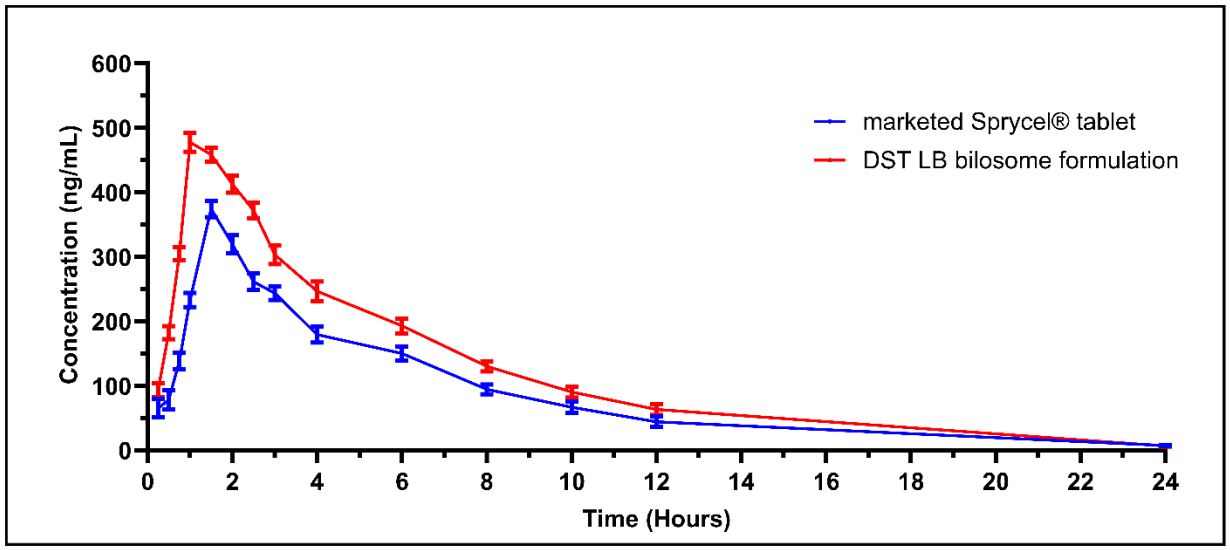

Figure 4: Assessment of the plasma levels of DST in rabbits for the standard tablet and DST-LB

4. Discussion

The findings of this study demonstrate that bilosome-based delivery of DST offers a promising strategy to overcome the solubility and bioavailability limitations associated with this BCS class II drug. The optimized bilosome formulation exhibited nanoscale particle size, narrow polydispersity, and a negative zeta potential, all of which are consistent with stable colloidal systems reported in previous nanocarrier studies.[17,33,46] The low PDI confirms the homogeneity of the vesicle population, ensuring reproducibility and consistent drug-release kinetics. In addition, the negative zeta potential imparted by bile salts provides electrostatic repulsion between vesicles, preventing aggregation and conferring colloidal stability during gastrointestinal transit. The high entrapment efficiency observed here aligns with earlier reports on bile salt-stabilized vesicles, where incorporation of bile salts enhanced drug loading and stability compared to conventional liposomes or niosomes.[18] Collectively, these parameters highlight the robustness of the formulation process and explain the improved dissolution and bioavailability observed in subsequent studies, while underscoring the superiority of bilosomes over conventional liposomes and niosomes, which often suffer from instability and heterogeneous particle populations.

Transmission electron microscopy confirmed the spherical morphology and bilayer structure, further supporting the successful assembly of bilosomes as described in prior work on

vesicular carriers.[16] The micromeritic properties of the lyophilized bilosome powder revealed significant improvements in flowability and compressibility compared to pure DST. These enhancements are particularly relevant for downstream processing, as poor flowability is a common challenge in the encapsulation of poorly soluble drugs.[47,48] The improved Carr's Index and Hausner's ratio values observed in this study are consistent with reports that nanocarrier-based solid dispersions can reduce interparticle cohesion and improve manufacturability.[11] Such improvements are critical for ensuring uniform capsule filling and content uniformity, both of which were achieved in the present work in accordance with pharmacopeial standards.

The dissolution study highlighted the distinct release behaviors of the bilosome capsule and the marketed DST tablet. While the marketed tablet achieved rapid dissolution consistent with USP specifications, the bilosome capsule exhibited a slower but sustained release profile, reaching near-complete release only after 50–60 minutes. This pattern aligns with previous studies on bilosome and niosome formulations, which have shown that the presence of bile salts and polymeric stabilizers modulates drug release kinetics.[10,49]

Kinetic modeling confirmed that the marketed tablet followed first-order release with a diffusional exponent (n) of 0.45, indicative of Fickian diffusion. In contrast, the bilosome capsule showed non-Fickian transport with an n value of 0.725. These findings are consistent with the mechanistic interpretations of the Korsmeyer–Peppas model, where values between 0.45 and 0.89 suggest a combination of diffusion and erosion processes.[50] Such controlled release behavior may be advantageous in reducing peak plasma fluctuations and prolonging therapeutic exposure, as has been demonstrated in other nanocarrier-based delivery systems.[51]

The pharmacokinetic evaluation in rabbits further substantiated the in vitro findings, showing that the bilosome formulation achieved a higher Cmax, a shorter Tmax, and a significantly greater AUC than the marketed tablet. These results indicate enhanced absorption and bioavailability, consistent with earlier reports that show nanocarrier systems improving the oral delivery of poorly soluble anticancer agents.[52,53] The relative bioavailability of more than 130% observed here is particularly noteworthy, as it surpasses improvements reported with amorphous solid dispersions and self-nanoemulsifying systems of DST.[10,11,54] The enhanced pharmacokinetic profile may be attributed to the ability of bile salts to facilitate membrane

permeation and protect the drug from degradation in the gastrointestinal tract, as previously described in bilosome research.[17]

Stability studies confirmed that the optimized bilosome formulation-maintained drug integrity under accelerated conditions, with degradation following first-order kinetics and an estimated shelf life of over two years at room temperature. This stability is consistent with the reported robustness of bilosomes, which are known to resist aggregation and degradation due to the electrostatic repulsion conferred by bile salts.[55] The ability to maintain stability without complex storage requirements enhances the translational potential of this formulation, particularly in regions with limited cold-chain infrastructure.

Overall, the results of this study align with and extend the growing body of literature supporting bilosomes as versatile nanocarriers for oral drug delivery. By improving solubility, modulating release kinetics, and enhancing bioavailability, bilosomes address key limitations of DST therapy. These findings suggest that bilosome-based formulations could provide a clinically meaningful alternative to conventional tablets, particularly for patients with variable gastric pH or those requiring more consistent systemic exposure. Future work should focus on establishing in vitro–in vivo correlations and conducting clinical evaluations to confirm the translational relevance of these promising preclinical results.

5. Conclusions

This study demonstrated the successful development and optimization of a DST-LB delivery system developed to overcome the poor aqueous solubility, pH-dependent absorption, and variable oral bioavailability of DST. The optimized formulation comprised uniform, spherical bilosomes with a well-defined bilayer structure in which bile salts and Soluplus® improved vesicle stability, drug encapsulation, and resistance to gastrointestinal degradation.The lyophilized bilosome powder exhibited valueable micromeritic properties, enabling successful capsule formulation.

In vitro dissolution studies showed a controlled and sustained release profile for the bilosome capsule compared with the rapid dissolution of the marketed immediate-release tablet,

corresponding with non-Fickian transport kinetics. In vivo pharmacokinetic evaluation in rabbits revealed improved oral absorption and increased systemic exposure for the bilosome formulation, indicating enhanced relative bioavailability and minimizing pH-dependent solubility limitations. Stability studies supported the formulation's practical potential.

Although the findings are encouraging, further studies are required to confirm clinical translation, including human pharmacokinetic evaluation, long-term safety assessment, and in vitro–in vivo correlation. Overall, the results show that bilosome-based delivery as a promising oral formulation for improving DST treatment.

6. Statements & Declarations

Conflicts of interest:

"The authors of this work have nothing to disclose."

Consent to participate

"Not applicable"

Data availability

"Data available upon request from the corresponding author."

Funding

"This study did not receive any funding in any form."

Ethics approval

"The study was approved by the Research Ethics Committee of the University of Baghdad, College of Pharmacy, with approval number "RECAUBCP22202505A," dated September 22, 2024."

Author Contribution

Ahmed Hamed Salman: Conceptualization, Methodology, Formal analysis, Investigation, Data curation, Writing – original draft, Visualization, Supervision.

Shaimaa Nazar Abd Alhammid: Methodology, Investigation, Validation, Resources, Writing – review & editing.

All authors have read and approved the final version of the manuscript and agree to be accountable for all aspects of the work.

7. References

1. Chen R, Chen B. The role of dasatinib in the management of chronic myeloid leukemia. *Drug Des Devel Ther* 2015;9:773-9. doi: 10.2147/dddt.S80207

2. Budha NR, Frymoyer A, Smelick GS, Jin JY, Yago MR, Dresser MJ, et al. Drug absorption interactions between oral targeted anticancer agents and ppis: Is ph-dependent solubility the achilles heel of targeted therapy? *Clin Pharmacol Ther* 2012;92(2):203-13. doi: 10.1038/clpt.2012.73

3. Korashy HM, Rahman AF, Kassem MG. Dasatinib. *Profiles Drug Subst Excip Relat Methodol* 2014;39:205-37. doi: 10.1016/b978-0-12-800173-8.00004-0

4. Dharani S, Rahman Z, Barakh Ali SF, Afrooz H, Khan MA. Quantitative estimation of phenytoin sodium disproportionation in the formulations using vibration spectroscopies and multivariate methodologies. *Int J Pharm* 2018;539(1-2):65-74. doi: 10.1016/j.ijpharm.2018.01.005

5. Eley T, Luo FR, Agrawal S, Sanil A, Manning J, Li T, et al. Phase i study of the effect of gastric acid ph modulators on the bioavailability of oral dasatinib in healthy subjects. *J Clin Pharmacol* 2009;49(6):700-9. doi: 10.1177/0091270009333854

6. Andersson P, Brisander M, Liljebris C, Jesson G, Lennernäs H. Severe impact of omeprazole timing on ph-sensitive dasatinib absorption: Unveiling substantial drug-drug interaction. *J Clin Pharmacol* 2025;65(5):588-97. doi: 10.1002/jcph.6173

7. Hofmann J, Bartůněk A, Hauser T, Sedmak G, Beránek J, Ryšánek P, et al. Dasatinib anhydrate containing oral formulation improves variability and bioavailability in humans. *Leukemia* 2023;37(12):2486-92. doi: 10.1038/s41375-023-02045-1

8. He S, Bian J, Shao Q, Zhang Y, Hao X, Luo X, Feng Y, Huang L. Therapeutic drug monitoring and individualized medicine of dasatinib: focus on clinical pharmacokinetics and pharmacodynamics. Front Pharmacol. 2021;12:797881. doi: 10.3389/fphar.2021.797881.

9. Lennernäs H, Liljebris C, Brisander M, Jesson G, Andersson P, Larfors G, et al. Xs004 dasatinib (xs004) improves variability and bioavailability in humans using amorphous solid dispersion formulation of dasatinib with potential implications for its clinical use. *Blood* 2022;140(Supplement 1):9652-3. doi: 10.1182/blood-2022-169884

10. Sokač K, Miloloža M, Kučić Grgić D, Žižek K. Polymeric amorphous solid dispersions of dasatinib: Formulation and ecotoxicological assessment. *Pharmaceutics* 2024;16(4):551. doi: 10.3390/pharmaceutics16040551

11. Dharani S, Mohamed EM, Khuroo T, Rahman Z, Khan MA. Formulation characterization and pharmacokinetic evaluation of amorphous solid dispersions of dasatinib. *Pharmaceutics* 2022;14(11). doi: 10.3390/pharmaceutics14112450

12. Mageshvaran D, Yadav S, Yadav V, Kuche K, Katari O, Jain S. Enhancing oral bioavailability of dasatinib via supersaturable snedds: Investigation of precipitation inhibition and ivivc through in-vitro lipolysis-permeation model. *Int J Pharm* 2025;668:125007. doi: 10.1016/j.ijpharm.2024.125007

13. Kaul M, Sanin AY, Shi W, Janiak C, Kahlert UD. Nanoformulation of dasatinib cannot overcome therapy resistance of pancreatic cancer cells with low lyn kinase expression. *Pharm Rep* 2024;76(4):793-806. doi: 10.1007/s43440-024-00600-w

14. Bahman F, Pittalà V, Haider M, Greish K. Enhanced anticancer activity of nanoformulation of dasatinib against triple-negative breast cancer. *J Pers Med* 2021;11(6):559. doi: 10.3390/jpm11060559

15. Conacher M, Alexander J, Brewer JM. Oral immunisation with peptide and protein antigens by formulation in lipid vesicles incorporating bile salts (bilosomes). *Vaccine* 2001;19(20-22):2965-74. doi: 10.1016/s0264-410x(00)00537-5

16. Al-Mahallawi AM, Abdelbary AA, Aburahma MH. Investigating the potential of employing bilosomes as a novel vesicular carrier for transdermal delivery of tenoxicam. *Int J Pharm* 2015;485(1-2):329-40. doi: 10.1016/j.ijpharm.2015.03.033

17. Abdel-moneum R, Abdel-Rashid RS. Bile salt stabilized nanovesicles as a promising drug delivery technology: A general overview and future perspectives. *J Drug Deliv Sci Technol* 2023;79:104057. doi: 10.1016/j.jddst.2022.104057

18. El-Nabarawi MA, Nabil SR, Faten F, and Nasralla SM. Bilosomes as a novel carrier for the cutaneous delivery for dapsone as a potential treatment of acne: Preparation, characterization and in vivo skin deposition assay. *J Liposome Res* 2020;30(1):1-11. doi: 10.1080/08982104.2019.1577256

19. Ahmed S, Aly KM, and Sayed S. Bilosomes as promising nanovesicular carriers for improved transdermal delivery: Construction, in vitro optimization, ex vivo permeation and in vivo evaluation. *Int J Nanomedicine* 2020;15:9783-98. doi: 10.2147/IJN.S278688

20. Palekar-Shanbhag P, Lande S, Chandra R, Rane D. Bilosomes: Superior vesicular carriers. *Current Drug Therapy* 2020;15(4):312-20. doi: 10.2174/1574885514666190917145510

21. Ahmad R, Srivastava S, Ghosh S, Khare SK. Phytochemical delivery through nanocarriers: A review. *Colloids and Surfaces B: Biointerfaces* 2021;197:111389. doi: 10.1016/j.colsurfb.2020.111389

22. Salman AH, Alhammid SNA, editors. Bilosome as a potential carrier for improving poor oral drug bioavailability. *J Emerg Med Trauma Acute Care* 2024;2024(6):17. doi: 10.5339/jemtac.2024.absc.17

23. Elebyary TT, Sultan A, Abu-Risha S, El Maghraby G. Bilosomes as oral drug delivery carrier. *Journal of Advanced Medical and Pharmaceutical Research* 2024;5(2):49-55.

24. Sankar DG, Rajeswari A, Babu AN, Krishna MV. UV-spectrophotometric determination of dasatinib in pharmaceutical dosage forms. *Asian J Chem* 2009;21(7):5777-9.

25. Maded ZK, Sfar S, Taqa GAA, Lassoued MA, Ben Hadj Ayed O, Fawzi HA. Development and optimization of dipyridamole- and roflumilast-loaded nanoemulsion and nanoemulgel for enhanced skin permeation: Formulation, characterization, and in vitro assessment. *Pharmaceuticals* 2024;17(6). doi: 10.3390/ph17060803

26. Al-Edhari GH, Al Gawhari FJ. Study the effect of formulation variables on preparation of nisoldipine loaded nano bilosomes. *Iraqi J Pharm Sci* 2023;32:271-82. doi: 10.31351/vol32issSuppl.pp271-282

27. Ali SK, Entidhar JA-A. Bilosomes as soft nanovesicular carriers for ropinirole hydrochloride: Preparation and in- vitro characterization. *Iraqi J Pharm Sci* 2023;32:177-87. doi: 10.31351/vol32issSuppl.pp177-187

28. Zolghadri S, Asad AG, Farzi F, Ghajarzadeh F, Habibi Z, Rahban M, et al. Span 60/cholesterol niosomal formulation as a suitable vehicle for gallic acid delivery with potent in vitro antibacterial, antimelanoma, and anti-tyrosinase activity. *Pharmaceuticals* 2023;16(12):1680. doi: 10.3390/ph16121680

29. Kaoud RM, Alwan MH, Amran M, Fawzi HA. Design and optimization of pantoprazole sodium mucoadhesive hydrogel microcapsules for the healing of peptic ulcers. *Pharmacia* 2024;71:1-14. doi: 10.3897/pharmacia.71.e118323

30. Lee MK, Kim MY, Kim S, Lee J. Cryoprotectants for freeze drying of drug nano-suspensions: Effect of freezing rate. *J Pharm Sci* 2009;98(12):4808-17. doi: 10.1002/jps.21786

31. Salman AH, Alkufi HK, Taher SS, Al-Mahmood S, Haiss MA. Response surface optimization and in vitro study of nasal solusomes nanovesicles for the bioavailability improvement and brain targetting of sumatriptan. *Epitheorese Klin Farmakol Farmakokinet* 2024;42:107-17. doi: 10.61873/RNYL6796

32. Maded ZK, Lassoued MA, Taqa GAA, Fawzi HA, Abdulqader AA, Jabir MS, et al. Topical application of dipyridamole and roflumilast combination nanoparticles loaded nanoemulgel for the treatment of psoriasis in rats. *Int J Nanomed* 2024;19:13113-34. doi: 10.2147/IJN.S492180

33. Lubna Abdalkarim S, Amer Sajjad K. Formulation and in-vitro evaluation of nanovesicles bilosomes loaded with ketoconazole. *Iraqi J Pharm Sci* 2025;34(1):156-64. doi: 10.31351/vol34iss1pp156-164

34. Al-Gharani H, Al-Kinani K, editors. Formulation and in vitro evaluation of acemetacin nanosuspension. *Iraqi J Pharm Sci* 2024;33:133-46.

35. Ramadhan SH, Al-Kinani KK. Statistical optimization and characterization of nimodipine transferosomes. *AlRafidain J Med Sci* 2024;7(1s):S77-S83. doi: 10.54133/ajms.v7i1(Special).1015

36. Ubhe AS. Imaging of liposomes by negative staining transmission electron microscopy and cryogenic transmission electron microscopy. In: D'Souza GGM, Zhang H, editors. Liposomes: Methods and protocols. New York, NY: Springer US; 2023. p. 245-51.

37. Luo FR, Yang Z, Camuso A, Smykla R, McGlinchey K, Fager K, et al. Dasatinib (bms-354825) pharmacokinetics and pharmacodynamic biomarkers in animal models predict optimal clinical exposure. *Clin Cancer Res* 2006;12(23):7180-6. doi: 10.1158/1078-0432.CCR-06-1112

38. Percie du Sert N, Ahluwalia A, Alam S, Avey MT, Baker M, Browne WJ, et al. Reporting animal research: Explanation and elaboration for the arrive guidelines 2.0. *PLOS Biology* 2020;18(7):e3000411. doi: 10.1371/journal.pbio.3000411

39. El-Hameed SA, Ibrahim I, Awadin W, El-Shaieb A. Assessment of single and combined administration of ubiquinone and lactoferrin on histopathology, ultrastructure, oxidative stress, and wnt4 expression gene induced by thioacetamide on hepatorenal system of adult male rats. *Beni-Suef Univ J Basic Appl Sci* 2024;13(1):41. doi: 10.1186/s43088-024-00494-w

40. Patel S, Patel S, Kotadiya A, Patel S, Shrimali B, Joshi N, et al. Age-related changes in hematological and biochemical profiles of wistar rats. *Lab Anim Res* 2024;40(1):7. doi: 10.1186/s42826-024-00194-7

41. Kassem MG, Ezzeldin E, Korashy HM, Mostafa GA. High-performance liquid chromatographic method for the determination of dasatinib in rabbit plasma using fluorescence detection and its application to a pharmacokinetic study. *J Chromatogr B Analyt Technol Biomed Life Sci* 2013;939:73-9. doi: 10.1016/j.jchromb.2013.09.012

42. FDA. Guidance for industry: Bioanalytical method validation and industry, us department of health and human services, food and drug administration, center for drug evaluationandresearch (cder),center forbiologics evaluation and research (cber), rockville, md 20857, USA; 2001.

43. ICH. March q2b validation of analytical procedures: Methodology, in: Proceeding of the international conference on harmonization, geneva, Switzerland; 1996.

44. Taher SS, Al-Kinani KK. In vivo brain pharmacokinetics of dolutegravir sodium-loaded nanostructured lipid carrier in situ gel: Comparative study with an intravenous drug solution. *AlRafidain J Med Sci* 2025;8(1):119-25. doi: 10.54133/ajms.v8i1.1692

45. Ashraf I, Hanna PA, Gad S, Abd-Allah FI, El-Say KM. Enhancing pharmacokinetics and pharmacodynamics of rosuvastatin calcium through the development and optimization of fast-dissolving films. *Pharmaceutics* 2023;15(11):2640. doi: 10.3390/pharmaceutics15112640

46. Zohdy MH, El-Kamel AH, Alseqely M, Bakr BA, Heikal LA. Bilosomal delivery of thymol-glycyrrhetinic acid: A multifaceted strategy to combat multidrug-resistant wound infections. *J Pharm Investig* 2025. doi: 10.1007/s40005-025-00741-x

47. El Menshawe SF, Aboud HM, Elkomy MH, Kharshoum RM, Abdeltwab AM. A novel nanogel loaded with chitosan decorated bilosomes for transdermal delivery of terbutaline sulfate: Artificial neural network optimization, in vitro characterization and in vivo evaluation. *Drug Deliv Transl Res* 2020;10(2):471-85. doi: 10.1007/s13346-019-00688-1

48. Kaurav H, Tripathi M, Kaur SD, Bansal A, Kapoor DN, Sheth S. Emerging trends in bilosomes as therapeutic drug delivery systems. *Pharmaceutics* 2024;16(6):697. doi: 10.3390/pharmaceutics16060697

49. Elebyary TT, Sultan AA, Abu-Risha SE, El Maghraby GM, Amin M. Bilosomal co-encapsulated tamoxifen and propranolol for potentiated anti-breast cancer efficacy: In vitro and in vivo investigation. *Pharmaceutics* 2025;17(1):123. doi: 10.3390/pharmaceutics17010123.

50. Siepmann J, Peppas NA. Modeling of drug release from delivery systems based on hydroxypropyl methylcellulose (HPMC). *Adv Drug Deliv Rev* 2001;48(2-3):139-57. doi: 10.1016/s0169-409x(01)00112-0

51. Bai X, Smith ZL, Wang Y, Butterworth S, Tirella A. Sustained drug release from smart nanoparticles in cancer therapy: A comprehensive review. *Micromachines* 2022;13(10):1623. doi: 10.3390/mi13101623

52. Alqosaibi AI. Nanocarriers for anticancer drugs: Challenges and perspectives. *Saudi J Biol Sci.* 2022;29(6):103298. doi: 10.1016/j.sjbs.2022.103298

53. Dey M, Das M, Chowhan A, Giri TK. Breaking the barricade of oral chemotherapy through polysaccharide nanocarrier. *Int J Biol Macromol* 2019;130:34-49. doi: 10.1016/j.ijbiomac.2019.02.094

54. Lennernäs H, Brisander M, Liljebris C, Jesson G, Andersson P. Enhanced bioavailability and reduced variability of dasatinib and sorafenib with a novel amorphous solid dispersion technology platform. *Clin Pharmacol Drug Dev.* 2024;13(9):985-99. doi: 10.1002/cpdd.1416

55. Ahmed S, Kassem MA, Sayed S. Bilosomes as promising nanovesicular carriers for improved transdermal delivery: Construction, in vitro optimization, ex vivo permeation and in vivo evaluation. *Int J Nanomedicine* 2020;15:9783-98. doi: 10.2147/ijn.s278688

List of tables

Table 1: Kinetic Modeling Parameters of In Vitro Dissolution Profiles for DST-LB Capsules and the Marketed Dasatinib Tablet

	Zero-order	**First-order**	**Higuchi**	**Korsmeyer-Peppas**	**N**
DST LB bilosome formulation	0.8611	0.9419	0.8613	0.9172	0.725
Marketed Sprycel® tablet	0.1357	0.9986	0.9307	0.9248	0.450

Table 2: Pharmacokinetics parameters of DST formulations

Paramters	**Standard tablet**	**DST-LB**
$T_{0.5}$ (hr)	4.38	3.69
T_{max} (hr)	1.5	1
C_{max} (ng/mL)	374.46	477.78
AUC $_{0\text{-}24hr}$ (ng/mL*h)	2061.72	2851.79
AUC $_{0\text{-}\infty}$ (ng/mL*h)	2107.67	2886.49
F $_{relative}$ (%) #	138.30	
F $_{relative}$ (%) $	136.95	

calculation based on AUC $_{0\text{-}24hr}$

$ calculation based on AUC $_{0\text{-}\infty}$